Reversibility of humidity effects in pentacene based organic thin-film transistor: experimental data and electrical modeling

W.Boukhili [a]*, M. Mahdouani[a], M. Erouel[b], J. Puigdollers[c], R. Bourguiga[a]

[a]Laboratoire de Physique des Matériaux : Structure et Propriétés, Groupe Physique des Composants et Dispositifs Nanométriques, Faculté des sciences de Bizerte, 7021 Jarzouna-Bizerte, Tunisia
[b]Lyon Institute of Nanotechnologies, CNRS and Ecole Centrale de Lyon, 36 Avenue Guy de Collongue, 69134 Ecully, France
[c]Department d'Enginyeria Electronica, Universitat Politecnica de Catalunya, C/Jordi Girona, Modul C4, Barcelona-08034, Spain

ABSTRACT

P-type organic thin-film transistors (OTFTs), in which the active semiconductor is made of pentacene with silicon dioxide as a gate insulator, were fabricated and characterized. The effects of humidity on the electrical characteristics of pentacene based thin-film transistors (pentacene-TFTs) in the linear and saturation regimes were investigated. We report the variation of the electrical parameters by relative humidity (RH) extracted from the experimental electrical characteristics current-voltage of pentacene-TFT devices. We show that the diffusion of water molecules (H_2O), the creation of acceptor states due to the presence of oxygen and the formation of clusters in the pentacene active layer considerably affect the stability and the performances of pentacene-TFTs. The degradation of electrical parameters of the pentacene- TFTs under relative humidity (RH) can be recovered with a simple pumping under vacuum (3×10^{-5} to 5×10^{-5}mbar). We also show that the changes introduced by the effects of humidity are reversible. Moreover the pentacene-TFT presents an intensive response for a high relative humidity (RH=57%), which could be used for a humidity detection device technology.

Keywords: humidity effects; electrical parameters degradation; stability of pentacene based TFTs; modeling

* Corresponding author: wboukehili@yahoo.fr
(Walid Boukhili)

1. Introduction

Organic Thin-Film Transistors (OTFTs) have received intensive interest because of their many advantages such as light-weight, low cost manufacture, structural flexibility and low temperature processing [1-3] that make them promising candidates in several areas of technology including gas sensors, smart cards, active-matrix displays and radio-frequency identification tags [4-8]. On the other hand, OTFTs provide multiple detection parameters like the inverse subthreshold swing (SS), the threshold voltage V_{th}, the field-effect mobility μ_{FET}, the current ratio I_{on}/I_{off} and the turn-on voltage V_{on} [9].The stability of organic transistors represents a major challenge that must be addressed for making this technology relevant and reliable. Therefore, the influences of environmental effects on the electrical stability of the OTFTs have been extensively studied in recent years [10-13]. The electrical performances of unencapsulated organic devices (including thin film transistors) degrade when exposed to humidity [14-16].The study of the influence of oxygen and water molecules on the characteristics of organic transistors is a crucial way for a best understanding of the interaction mechanisms between the organic active layer and these chemical species and their consequences on the performance of the device. Furthermore, the influences of impurities and structural properties of the organic semiconductor films have been widely investigated [17-19]. In addition, the progress and the improvement in the sensors technology based on OTFTs, such as sensors of temperature, pressure, gas, humidity and photodetectors are directly related to the response and the sensitivity of the active layer of the transistor to external disturbances such as the temperature, illumination and humidity.

The main aim of this work is to report the effects of the humidity on the electrical stability of pentacene based TFTs in the linear and the saturation regimes. Accordingly, the electrical parameters characterizing the transistors were extracted from experimental data in different measurement conditions. In particular we have characterized the pentacene-TFTs under vacuum and under different relative humidity (RH) conditions. RH is defined as the ratio of the water vapor density (mass per unit volume) to the saturation water vapor density usually expressed in percent. Electrical characterization was done under vacuum (3×10^{-5} to 5×10^{-5} mbar), under different relative humidity (RH=3% and RH=57%), and finally under nitrogen (N_2) +RH=3%. In the last experiment, the sample was subjected to a vacuum process for 48 hours in order to study the reversibility of the degradation. Finally, we have developed an

analytical model to reproduce the experimental output characteristics for two measurement conditions (under vacuum and under RH=57%).

2. Experimental details

Fig.1 shows the schematic structure of the fabricated pentacene-TFTs used in the present work. We have used a bottom-gate top-contact structure. A highly p-doped crystalline silicon wafer (p-Si) was used as a substrate. The Si substrate was cleaned sequentially by acetone, methanol, and de-ionized water in an ultrasonic bath for 10 min at each step. The SiO_2 layer of 300nm was grown on the p-Si substrate in a furnace at 1000°C for 2hours and it was used as the gate-insulator. Then, a pentacene ($C_{22}H_{14}$) layer (40 nm thick) was deposited on top of the SiO_2 by thermal evaporation in a high vacuum chamber (3×10^{-6} mbar). Finally, 80 nm gold (Au) source and drain electrodes were deposited by thermal evaporation under high vacuum (10^{-8} mbar) to obtain high quality ohmic contacts with the pentacene thin film. The deposition rates and the thicknesses of the pentacene and metallic layers were determined by a quartz balance. The channel length (L) and width (W) were 50µm and 3760µm, respectively, and they were defined using a shadow mask during the gold (Au) evaporation. The electrical characteristics and environmental stability of pentacene-TFTs were measured by using a manual Karl Süss probe and two programmable source-meters (Keithley 2400). The characterization under relative humidity (RH) was carried out by using a humidification system constituted of a water reservoir, three valves and two mass flow controllers enabling a gas flow regulation between 0 and 200sccm. The measured relative humidity at the output of the system varies between 2% and 79%.

3. Results and discussion

3.1. Output characteristics of the pentacene based TFT under different measuring condition

Figs. 2(a)-2(e) show the output characteristic (I_D vs. V_D) curves of the fabricated pentacene-TFTs. The drain voltage (V_D) was varied from 0 to -80V in -1V increments at different gate voltages (V_G) ranging from 0 to -40V with -10V increments. The measurements were carried out using five different conditions. Firstly, the measurement was made under vacuum (3×10^{-5} to 5×10^{-5} mbar) and repeated again after 30 minutes under RH=3%. A third measurement was carried out after 30 minutes under a high RH level (RH=57%), followed by a measurement

after 30 minutes, in which the device was subjected to a flow of dry nitrogen in order to reduce the relative humidity toward RH=3%. Finally, we have made the measurement under vacuum after two days of pumping.

The resulting output characteristics of the pentacene-TFTs (Figs. 2(a)-2(e)) show a typical p-channel operation. All the transistors showed a clear linear increase of the drain current at low drain voltages (linear regime), followed by a saturation at larger voltages (saturation regime) for all the experimental conditions. An exception was observed for the transistors subjected to a RH = 57% (fig.2.c). For these transistors the saturation of the drain current was not observed. This behavior is attributed to the diffusion of H_2O molecules in the thin film of pentacene which increases the current I_{off} and prevents the saturation of the output characteristics [20]. Moreover, we note that the drain current increases by increasing the gate voltage in all the measurement conditions.

3.2. Transfer characteristics of the pentacene TFT in linear and saturation regime

3.2.1. In linear regime

In Fig.3, we represent the transfer characteristics ($|I_D|$ vs.V_G) for all the measurement conditions in the linear regime for a fixed drain voltage (V_D= - 10V) and by varying the gate voltage (V_G) of -50 to 50Vwith 0.2V increments. We note that there is a significant decrease in the absolute value of the drain current of pentacene TFT with the humidity for high negative gate voltages.

3.2.1. 1. Series resistance of the pentacene TFT

The electrical performance of the OTFTs was mainly limited by the resistance effects. These effects are directly related to the increase of the charge carrier density in the channel of the transistor. Several methods have been developed for the extraction of the series resistance in OTFTs [21-22]. In the linear regime, the transconductance g_m can be defined as [23]:

$$g_m = \left[\frac{\delta I_D}{\delta V_G}\right]_{V_{D=cte}} = \frac{W}{L}\mu_{FET,lin}C_iV_D \qquad (1)$$

where Wand L are the channel's width and length of the transistor, respectively, C_i is the insulator capacitance (per unit area), V_D is the drain voltage fixed to -10V and $\mu_{FET,lin}$is the

field effect mobility in the linear regime that can be calculated through the following equation [24]:

$$\mu_{FET,lin} = \frac{L}{C_i V_D W}\left[\frac{\delta I_D}{\delta V_G}\right]_{V_{D=cte}} = \frac{L}{C_i V_D W} g_m \quad (2)$$

In this regime, the expression of the series resistance of the pentacene-TFT is defined as follows:

$$R_S = \frac{1}{g_d} - \frac{L}{W C_i \mu_{FET,lin}(V_G - V_{th})} \quad (3)$$

where g_d is the conductance $g_d=\left[\frac{\delta I_D}{\delta V_D}\right]_{V_{G=cte}}$, since in the linear regime we work at low drain voltage (V_D = -10V) we can approximate the numerical derivative of the drain current on the drain voltage to the ratio of these quantities: $g_d= \left[\frac{\delta I_D}{\delta V_D}\right]_{V_{G=cte}} = \frac{I_D}{V_D}$[23].

The other parameters were defined previously.

Fig.4 shows the experimentally values of the series resistance R_s as a function of the gate voltage for the five measurement conditions. It is clear that the series resistance decreases rapidly for negative gate voltages because the increase in the density of charge introduced in the conducting channel. Furthermore, in the inset we have depicted the series resistance for positives gate voltages. It is observed that for positive gate voltages the series resistance increases with increasing humidity.

The pentacene compound contains an abundance of hole charge carriers which categorizes it as a p-type semiconductor. For this reason, it is necessary to apply a negative gate voltage to increase the density of holes in the conducting channel. In this case, i.e. for negative gate voltages, we see that the series resistance decreases by increasing humidity. On the contrary, for the positive gate voltages, the series resistance increases with the humidity. This behavior could be explained by the chemical nature of the polar water molecules [10, 11, 20].

3.2.2. In saturation regime

Fig.5 (a) shows the transfer characteristics ($|I_D|$ vs. V_G) of our pentacene TFT in the saturation regime at V_D= -70V for the five measurement conditions. We note that the absolute value of the drain current increases as the humidity increases. At V_G = - 40V, the increase is approximately 40% higher between the first measurement (under vacuum) and the third measurement (under RH = 57%). This behavior can be explained by the fact that the

pentacene reacts with absorbed H_2O molecules and forms clusters of pentacene/ $(H_2O)_n$. These clusters have a role as a p-type doping and, as a consequence, the drain current increases [25]. For the purpose of eliminating the effect of the H_2O molecules and oxygen, as well as the clusters that are unstable under vacuum, the transistor was exposed to a pumping step for 48 hours under vacuum (3×10^{-5} to 5×10^{-5}mbar). After this treatment, the drain current decreases and comes back to the initial characteristics.

4. Extraction of key parameters of the pentacene TFT from experimental data

4.1. The threshold voltage V_{th} and the trapped charge density $N_{trap.charge}$

The threshold voltage (V_{th}) has been extracted from a plot of the square root of $|I_D|$versus V_G. In particular V_{th} can be estimated from the intersection of the tangent of the linear part of the plot of the square root of $|I_D|$with the axis of gate voltages (Fig.5 .b). Under vacuum (3×10^{-5} to 5×10^{-5} mbar), the determined value of V_{th} was 10V. After 30 minutes under nitrogen at a RH = 3%, V_{th} shifts to 29.8V. Afterwards, the measurement is carried out under RH =57%, and the V_{th} reaches a maximum value of 67V and for the measurement after 30 minutes under RH = 3%, the V_{th} decreases to 45V. Finally, under vacuum after 2 days of pumping, the V_{th} decreases to a value 8V similar to the one obtained at the initial state (under vacuum). We conclude that the relatively humidity affects the stability of pentacene TFT, in particular shifting the V_{th} to higher positive values. This shift of the threshold voltage is generally attributed to the creation of an electric field around the insulator / pentacene interface due to the presence of trapped charges [26, 27].

Generally, the variation of the threshold voltage in OTFTs is directly related to the trapped charge density in the insulator /organic semiconductor interface [28].The trapped charge density at the insulator/organic TFTs can be determined by the following relation [29]:

$$N_{trap.charge} = \frac{|\Delta V_{th}|Ci}{q} \quad (4)$$

where C_i is the insulator capacitance per unit area, ΔV_{th} the measured shift in the threshold voltage and q is the electronic charge.

4.2. Extraction of the inverse subthreshold swing (SS), the interface trap density D_{it}, the turn-on voltage V_{on} and the ratio current I_{on}/ I_{off}

The inverse subthreshold swing (SS), related to the sharpness between the off and on state, can be determined by the following relation [30]:

$$SS = \left[\frac{dlog(I_d)}{dV_g}\right]^{-1} \quad (5)$$

The fact that the SS values changes with humidity suggests the existence of trap sites located at the interface of the insulator/pentacene. It is well known that the quality of this interface plays a decisive role in the functional performance of the OTFTs. The density of the interface trap in TFT devices can be determined by the following relation [31-32]:

$$D_{it} = \left[\frac{SSlog(e)}{KT/q} - 1\right]\frac{C_i}{q} \quad (6)$$

Where T is the temperature, k is Boltzmann's constant and q is the electronic charge.
Table 1 shows that there is a shift of the turn-on voltage V_{on} toward positive values and an increase in the SS values with increasing RH. Indeed, the degradation of V_{on} and SS is directly linked to the oxygen molecules that are incorporated into the film of pentacene by creating acceptor states [33]. Another important parameter characterizing the performance of TFT devices is the current ratio I_{on}/ I_{off}. This ratio describes the ability of a device to switch from the on to the off state. The values of I_{on}, I_{off} and V_{on} are extracted by tracing the variation of the drain current in logarithmic scale versus the gate voltage in the saturation regime (log $|I_D|$ vs.V_G). In fig.5.c, we illustrated the method to determine these parameters for the pentacene-TFTs measured under vacuum. The same procedure was repeated for the other measurement conditions.

All the electrical parameters that could be extracted from the measured curves are summarized in table 1, such as the threshold voltage, the trapped charge density, the inverse subthreshold swing, the interface trap density, the turn-on voltage and the on/off ratio current.

4.3. Saturation mobility μ_{sat}

The field-effect mobility is an important parameter of the transistor, which describes the ease of the charge carriers to move inside the active layer under the influence of an electric field. This parameter is thus directly connected to the switching speed of the device.

In the saturation regime and for a constant drain voltage V_D= -70V, the slope of the square root of $|I_D|$versus V_G in the saturation regime allows deducing the mobility using the following relation:

$$\mu_{sat} = \frac{2L}{WC_i}\left(\frac{\partial\sqrt{I_D}}{\partial V_G}\right)^2 \quad (7)$$

Fig. 6 shows the extracted saturation mobility from the plot of the square root of $|I_D|$ versus V_G in the saturation regime measured in the different conditions. We found that the saturation mobility decreases with increasing relative humidity.

This degradation of mobility is attributed to several effects introduced by humidity within the active layer of pentacene. Indeed, the decrease in the saturation mobility could be attributed to polar water molecules that diffused into the grain boundaries of the pentacene polycrystalline structure and interact with holes charge carriers. Therefore, the increased potential barriers make more difficult the transport of charge carriers in the conductive channel of the device [34-36]. Thus, the polar water molecules can interact with the charges in the channel and reduce the mobility.

5. Modeling of output characteristics of pentacene based TFT under vacuum and under RH=57%

The electrical characteristics of OTFTs have been extensively simulated using the same models used for standard inorganic Metal-Oxide Semiconductor Field-Effect Transistors (MOSFETs). However, organic devices show several differences with respect to their inorganic counterparts. In particular, in organic devices of the charge carrier conduction at the metal/ semiconductor junction and the low intrinsic conductivity of organic semiconductors play an important role. These differences should be added in the numerical or analytical models when analyzing organic TFTs [37-39].

Taking into account the current due to the contribution of the intrinsic conductivity of pentacene, the total drain current in the linear and saturation regimes can be expressed as follows:

$$I_D = I_{accum} + I_{leakage} \tag{8}$$

where I_{accum} is the contribution from the accumulation of majority charge carriers at the conductive channel of the TFT and $I_{leakage}$ is the leakage current due to the intrinsic conductivity of pentacene. Leakage current can be determined by the following equation [40]:

$$I_{leakage} = \sigma_0 V_D \tag{9}$$

where $\sigma_0$is the minimum leakage current and V_D is the drain voltage.

Taking into account the conductive channel length modulation by the drain voltage and the series resistance of the drain and source electrodes, the effective conductivity of the majority charge carriers in the conduction channel may be expressed as follows:

$$g_{ch,eff} = \frac{g_{chint}}{1+g_{chint}((R_S+R_D))} \tag{10}$$

where $R_s = R_S+R_D$ is the series resistance between source and drain electrodes and g_{chint} is the intrinsic conductivity of the channel. The g_{chint} value can be calculated from this equation:

$$g_{chint} = \left(\frac{W}{L} C_i\right) \mu_{FET}(V_G - V_{th}) \tag{11}$$

Then, the current attributed to the accumulated charge carriers I_{accum} can be expressed as:

$$I_{accum} = g_{ch,eff}\, V_{D,eff}(1 + \lambda V_D) \tag{12}$$

where $\lambda$is the channel length modulation parameter and $V_{D,eff}$ is the effective drain voltage which it is given by [41]:

$$V_{D,eff} = \frac{V_D}{\left[1+\left(V_D/V_{D,sat}\right)^m\right]^m} \tag{13}$$

where m is a control transition parameter from the linear to the saturation regime. The m parameter is also known as the knee shape parameter.

$V_{D,\,sat}$ is the saturation voltage that is given by:

$$V_{D,sat} = \alpha_s V_{G,sat} = \alpha_s . V_{th}\left[1 + \frac{V_G - V_{th}}{2V_{th}} + \sqrt{\delta^2 + \left(\frac{V_G - V_{th}}{V_{th}} - 1\right)^2}\right]$$

By substituting $V_{D,eff}$ that is given previously by (13) in (12), we obtain the following expression for I_{accum}:

$$\mathrm{I_{accum}} = \frac{g_{ch,eff} V_D (1+\lambda V_D)}{\left[1+\left(V_D / V_{D,sat}\right)^m\right]^{\frac{1}{m}}} \quad (14)$$

Therefore, the final expression of the current is given by:

$$I_D = \frac{g_{ch,eff} V_D (1+\lambda V_D)}{\left[1+\left(V_D \Big/ \left(\alpha_s . V_{th}\left[1+\frac{V_G - V_{th}}{2\,V_{th}} + \sqrt{\delta^2 + \left(\frac{V_G - V_{th}}{V_{th}} - 1\right)^2}\right]\right)\right)^m\right]^{1/m}} + \sigma_0 V_D \quad (15)$$

Where α_s is the saturation modulation parameter and δis the transition width parameter.

Fig.7 shows a graphical method to extract the different parameters indicated in the final expression of the drain current: R_s, m, ΔI, $I_{D,sat}$, $g_{ch,sat}$ and λ[39]. The parameter m is determined using the following relation:

$$m = \frac{ln(2)}{ln\left(\frac{I_{D,sat}}{I_{D,sat} - \Delta I}\right)} \quad (16)$$

where ΔI is the difference between the saturation current $I_{D,\,sat}$ and the current value obtained by the projection on the current-voltage curve of the intersection of the two slopes of the current-voltage characteristics in the linear and saturation regimes (fig. 7).

The parameter λ was determined from the slope of the current-voltage characteristic in the saturated state as shown in figure 7 using the following equation:

$$g_{ch.sat} = \lambda I_{D,sat}$$

The set of parameters that gave a good agreement between the experimental data and those simulated by the equation (15) are summarized in table 2.

The absence of the transition between the linear regime and the saturation regime in the output characteristics measured under a high RH level (RH=57% fig.2.c) is well confirmed by the proposed model used to simulate the electrical characteristics of the pentacene TFTs according to the values of the parameter (m) which controls the transition between the linear and the saturation regimes. Indeed, under vacuum where we have a good transition between the two regimes this parameter is higher (m= 3.48) than that obtained for the measurement under RH= 57% (m=0.238).

6. Conclusion

The analysis of the experimental curves obtained on the pentacene based TFTs measured in different humidity conditions have confirmed the effects of relative humidity on the electrical characteristics of TFTs in the linear and in the saturation regimes. This study enabled us to determine the electrical parameters of the fabricated pentacene-TFTs in different measurement conditions. We demonstrated that the electrical parameters such as the threshold voltage, trapped charge density, inverse subthreshold swing, interface trap density, turn-on voltage, current ratio and saturation mobility are degraded by humidity. Furthermore, we have investigated the influence of the series resistance R_s on the drain current in the linear regime for different humidity conditions. We found that R_s increases with RH only for positives gate voltages. We have also been able to reproduce the output electrical characteristics of our pentacene-TFTs by developing an analytical model. The obtained results are in good agreement with the experimental results for both vacuum and RH=57% conditions.

References

[1] C.L. Fan, P.C. Chiu, C.C. Lin, IEEE Electron Dev. Lett. 31 (2010) 1485.

[2] C.L. Fan, Y.Z. Lin, W.D. Lee, S.J. Wang, C.H. Huang, Org. Electron. 13 (2012) 2924.

[3] C.Y. Wei, F. Adriyanto, Y.J. Lin, Y.C. Li, T.J. Huang, D.W. Chou, Y.H. Wang, IEEE Electron Dev. Lett. 30 (2009) 1039.

[4] B. Crone, A. Dodabalapur, A. Gelperin, L. Torsi, H.E. Katz, A.J. Lovinger, Z. Bao, Appl. Phys. Lett. 78 (2001) 2229.

[5] M.C. Hamilton, J. Kanicki, IEEE J. Sel. Topics. Quantum Electron. 10 (2004) 840.

[6] H.E. Katz, Chem. Mater. 16 (2004) 4748.

[7] H. Nakanotani, S. Akiyama, D. Ohnishi, M. Moriwake, M. Yahiro, T. Yoshihara, S. Tobita, C. Adachi, Adv. Funct. Mater. 17 (2007) 2328.

[8] M. Berggren, D. Nilsson, N.D. Robinson, Nature Mater. 6 (2007) 3.

[9] L. Torsi, A. Dodabalapur, L. Sabbatini, and P. G. Zambonin, Sens. Actuatr B., vol. 67 (2000) 312–316.

[10] R. Ye, M. Baba, K. Suzuki, Y. Ohishi, K. Mori, Thin Solid Films 464–465 (2004) 437–440.

[11]Jaehoon Park, Lee-Mi Do, Jin-Hyuk Bae, Ye-Sul Jeong, Christopher Pearson, Michael C. Petty, Organic Electronics 14 (2013) 2101–2107.

[12] Z. Zhu, J. Mason, R. Dieckmann, G.G. Malliaras, Appl. Phys. Lett. 81 (2002) 4643.

[13] I. Murtaza, Kh S. Karimov1; 2, Zubair Ahmad, I. Qazi, M. Mahroof-Tahir, T. A. Khan, and T. Amin, 31 (2010) 5.

[14] C.R. Kagan, A. Afzali, T.O. Graham, Appl. Phys. Lett. 86 (2005) 193505.

[15] D. Knipp, A. Benor, V. Wagner, T. Muck, J. Appl. Phys. 101 (2007) 044504.

[16] S. Hong, J. Choi, Y. Kim, IEEE Trans. Electron Devices 55 (2008) 3602.

[17] H. Sirringhaus, Adv. Mater. 21 (2009) 3859.

[18] K.K. Ryu, I. Nausieda, D.D. He, A.I. Akinwande, V. Bulovic´ , C.G. Sodini, IEEE Trans. Electron Devices 57 (2010) 1003.

[19] S. Yang, C.-S. Hwang, J.-I. Lee, S.-M. Yoon, M.-K. Ryu, K.-I. Cho, S.-H. Ko Park, S.-H. Kim, C.-E. Park, J. Jang, Appl. Phys. Lett. 98 (2011) 103515.

[20] S. Hoshino, M. Yoshida, S. Uemura, T. Kodzasa, N. Takada, T. Kamata, K. Yase, J. Appl. Phys. 95 (2004) 5088.

[21] R. Bourguiga. M. Mahdouani, S. Mansouri, and G. Horowitz, Eur. Phys. J. Appl. Phys. 39 (2007) 7–16.

[22] Yow-Jin Lin, Bo-Chieh Huang, Microelectronic Engineering, 103 (2013) 76-78.

[23] G.Horowitz, R. Hajlaoui, D. Fichou, A. El Kassmi, J. Appl. Phys. 85 (1999) 6.

[24] R. Bourguiga, F. Garnier, G. Horowitz, R. Hajlaoui, P. Delannoy, M. Hajlaoui, H. Bouchriha, Eur. Phys. J. Appl. Phys. 14 (2001) 121.

[25] R. Ye, M. Baba, K. Suzuki, Y. Ohishi, K. Mori, Thin Solid Films 464 (2004) 437.

[26] W. A. Schoonveld, J. B. Oostinga, J. Vrijmoeth, T. M. Klapwijk, Synthetic metals 101(1999) 608.

[27]S. M. Sze, Physics of Semiconductor Devices (Wiley-Interscience, New York, (1981).

[28] A. Bolognesi, M. Berliocchi, M. Manenti, A.D. Carlo, P. Lugli, K. Lmimouni, C. Dufour, IEEE Trans. Electron Devices 51 (2004) 1997.

[29] K.P. Pernstich, S. Haas, D. Oberhoff, C. Goldmann, D.J. Gundlach, B. Batlogg, A.N. Rashid, G. Schitter, J. Appl. Phys. 96 (2004) (11) 6431.

[30] L.A. Majewski, M. Grell, Synth. Met. 151 (2005) 175.

[31] G. Horowitz, Adv. Funct. Mater. 13 (2003) 53.

[32] R.N. Christopher, C.D. Frisbie, D.A. da Silva Filho, J.L. Bredas, C.E. Paul, R.M. Kent, Chem. Mater. 16 (2004) 4436.

[33] D. Knipp, T. Muck, A. Benor, V. Wagner, Journal of Non-Crystalline Solids, 352 (2006) 1774.

[34] D. H. Dunlap, P. E. Parris, and V. M. Kenkre, Phys. Rev. Lett. 77(1996) 542.

[35] D. J. Gundlach, T. N. Jackson, D. G. Schlom, and S. F. Nelson, Appl. Phys. Lett. 74 (1999) 3302.

[36] D. Zou and T. Tsutsui, J. Appl. Phys. 87 (2000) 1951.

[37] P.V. Necludov, M. Shur, Solid-State Electron. 47 (2003) 259–262.

[38] H. Klauk, G. Schmid, W. Radlik, W. Weber, L. Zhou, C.D. Shraw, J.A. Nichols, T. Jackson, Solid-State Electron. 47 (2003) 297–301.

[39]S. Mansouri, G.Horowitz, R.Bourguiga, Synthetic Metals, 160 (2010) 1787–1792.

[40] Chen Yingping, Shang Liwei, Ji Zhuoyu, Wang Hong, Han Maixing, Liu Xin, Liu Ming, Journal of Semiconductors 32 (2011) 11.

[41] M. Bartzsch , H. Kempa, M. Otto , A. Hübler, D. Zielke, Organic Electronics 8 (2007) 431–438.

Figures captions

Figure. 1. Schematic diagram of a bottom-gate top-contact pentacene-TFT.

Figures.2 (a)–2(e). Output characteristic curves of pentacene-TFTs under different measurement conditions.

Figure.3. Transfer characteristics ($|I_D|$ versus V_G plots) measured in the linear regime at V_D = -10*V* under different measurement conditions.

Figure.4. Series resistance of the pentacene -TFTs vs. V_G in the linear regime. The inset depicts the series resistance for positives gate voltages.

Figures. 5(a)-5(b). (a) Transfer characteristics ($|I_D|$ and square root of $|I_D|$ versus V_G plots measured in the saturation regime at V_D = -70V under different measuring condition. **(b)** Square root of $|I_D|$ from which the threshold voltage was determined for each measurement step.

Figure. 5(c) Extraction method of the parameters: the turn-on voltage and the ratio current.

Figure.6. The saturation mobility versus measurement conditions.

Figure.7. Graphical procedure parameters extraction from the output characteristics of the pentacene-TFTs.

Figure.8. The good agreement between experimental (circle line) and that obtained from Eq. 15 (full line) output characteristics of pentacene-TFT: **(a)** under vacuum and (**b)** RH=57%.

Tables captions

Table 1. Experimental electrical parameters of pentacene-TFTs for all the measurement conditions.

Table 2. Parameter values that give a good agreement between the measured characteristics and those obtained by the equation (15).

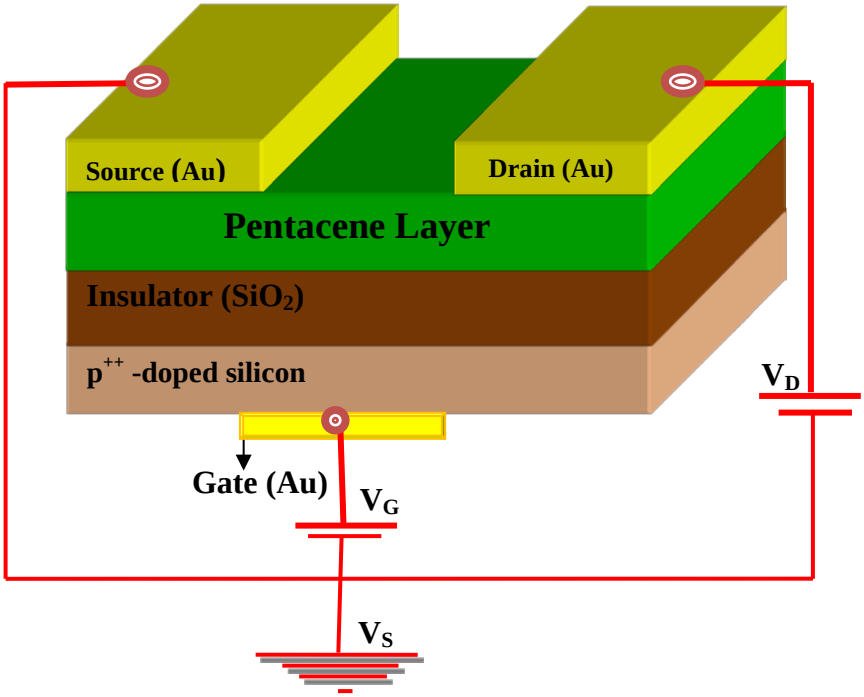
Source (Au)
Drain (Au)
Pentacene Layer
Insulator (SiO_2)
p^{++} -doped silicon
Gate (Au)
V_D
V_G
V_S

Figure.1.

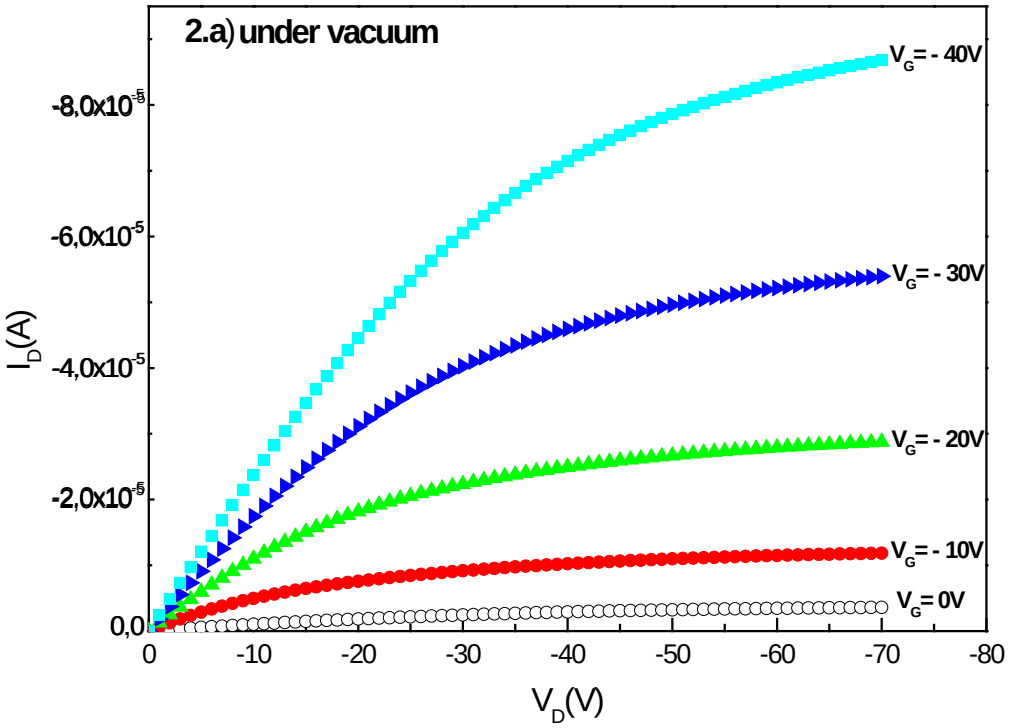
2.a) under vacuum
V_G= - 40V
V_G= - 30V
V_G= - 20V
V_G= - 10V
V_G= 0V
-8,0x10^-5
-6,0x10^-5
-4,0x10^-5
-2,0x10^-5
0,0
I_D(A)
0
-10
-20
-30
-40
-50
-60
-70
-80
V_D(V)

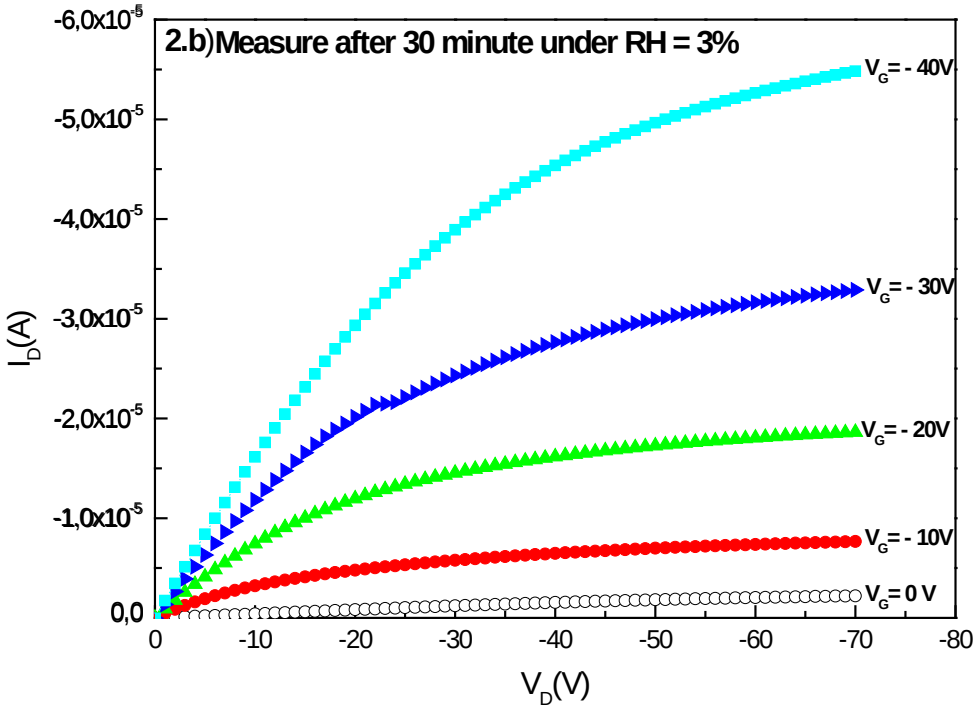
2.b)Measure after 30 minute under RH = 3%
V_G= - 40V
V_G= - 30V
V_G= - 20V
V_G= - 10V
V_G= 0 V
-6,0x10^-5
-5,0x10^-5
-4,0x10^-5
-3,0x10^-5
-2,0x10^-5
-1,0x10^-5
0,0
I_D(A)
0
-10
-20
-30
-40
-50
-60
-70
-80
V_D(V)

Figures.2. (a)-(b)

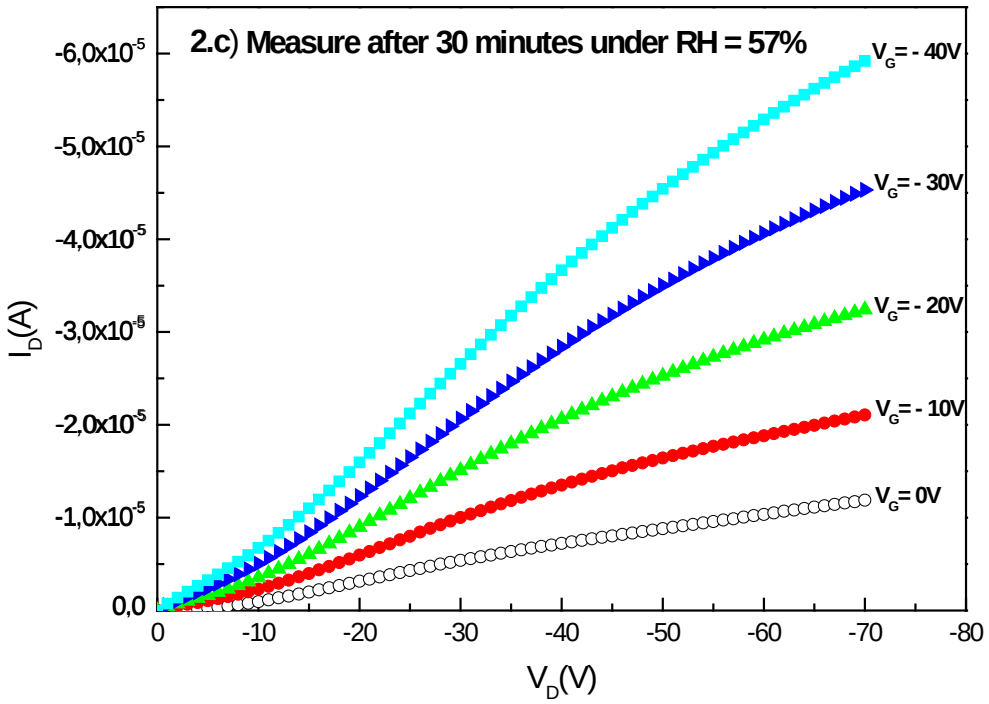
2.c) Measure after 30 minutes under RH = 57%
V_G= - 40V
V_G= - 30V
V_G= - 20V
V_G= - 10V
V_G= 0V
I_D(A)
-6,0x10^{-5}
-5,0x10^{-5}
-4,0x10^{-5}
-3,0x10^{-5}
-2,0x10^{-5}
-1,0x10^{-5}
0,0
0
-10
-20
-30
-40
-50
-60
-70
-80
V_D(V)

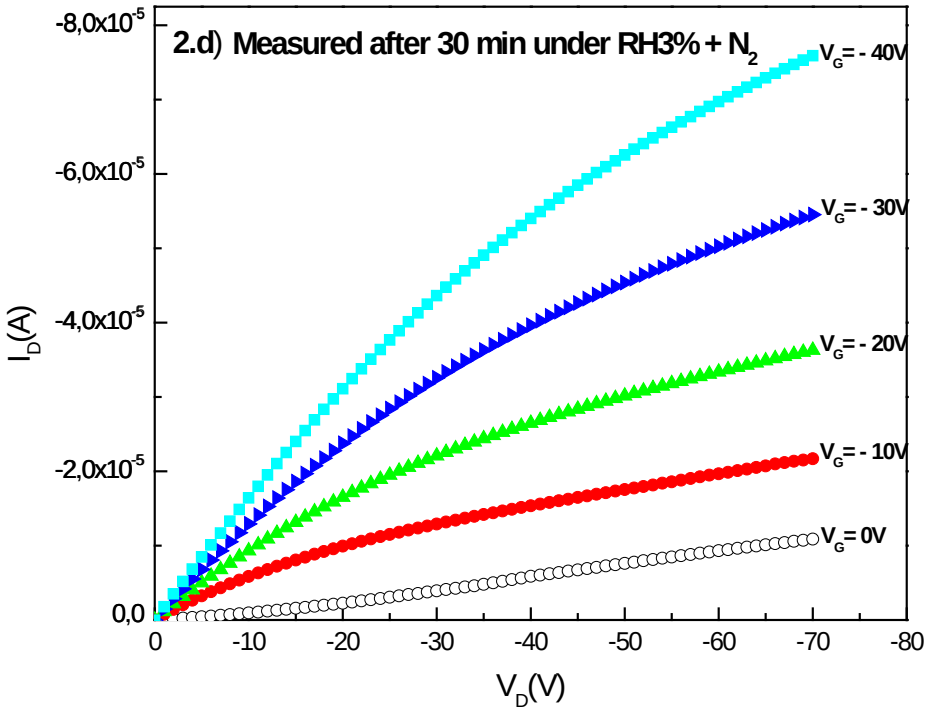
2.d) Measured after 30 min under RH3% + N_2
V_G= - 40V
V_G= - 30V
V_G= - 20V
V_G= - 10V
V_G= 0V
I_D(A)
-8,0x10^{-5}
-6,0x10^{-5}
-4,0x10^{-5}
-2,0x10^{-5}
0,0
0
-10
-20
-30
-40
-50
-60
-70
-80
V_D(V)

Figures.2. (c)-(d)

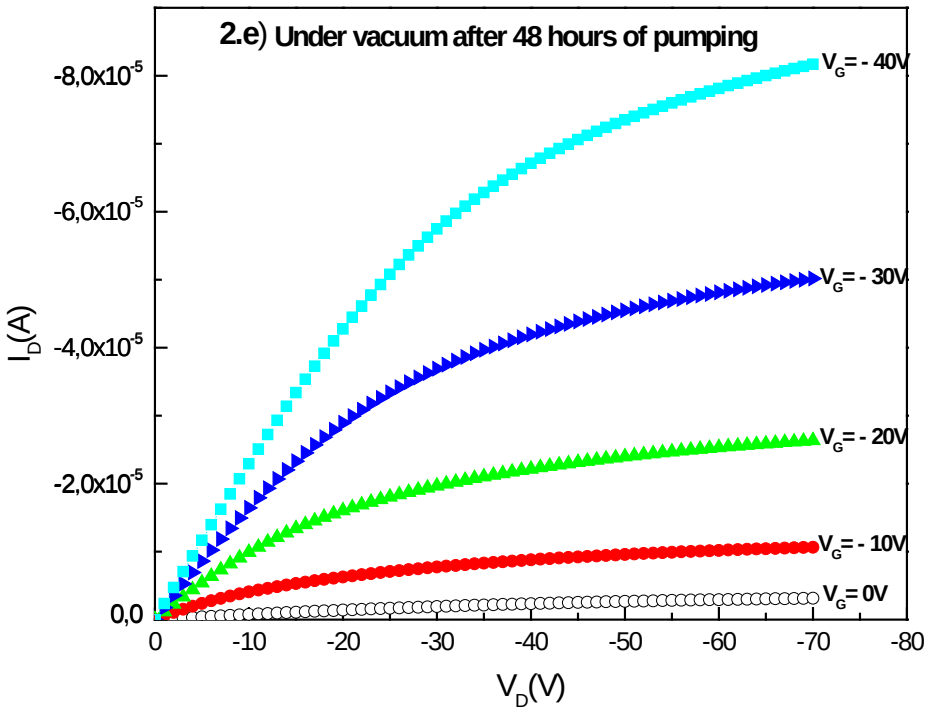
2.e) Under vacuum after 48 hours of pumping
-8,0x10-5
-6,0x10-5
-4,0x10-5
-2,0x10-5
0,0
ID(A)
0
-10
-20
-30
-40
-50
-60
-70
-80
VD(V)
VG= - 40V
VG= - 30V
VG= - 20V
VG= - 10V
VG= 0V

Figures.2. (e).

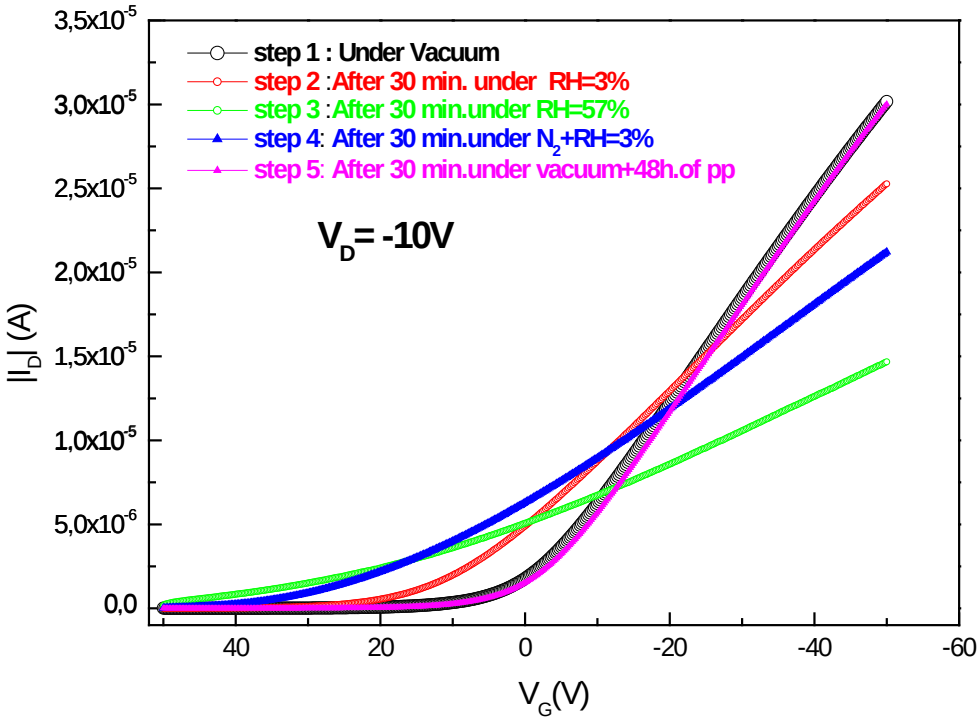
step 1 : Under Vacuum
step 2 :After 30 min. under RH=3%
step 3 :After 30 min.under RH=57%
step 4: After 30 min.under N2+RH=3%
step 5: After 30 min.under vacuum+48h.of pp
VD= -10V
|ID| (A)
VG(V)
3,5x10-5
3,0x10-5
2,5x10-5
2,0x10-5
1,5x10-5
1,0x10-5
5,0x10-6
0,0
40
20
0
-20
-40
-60

Figures.3

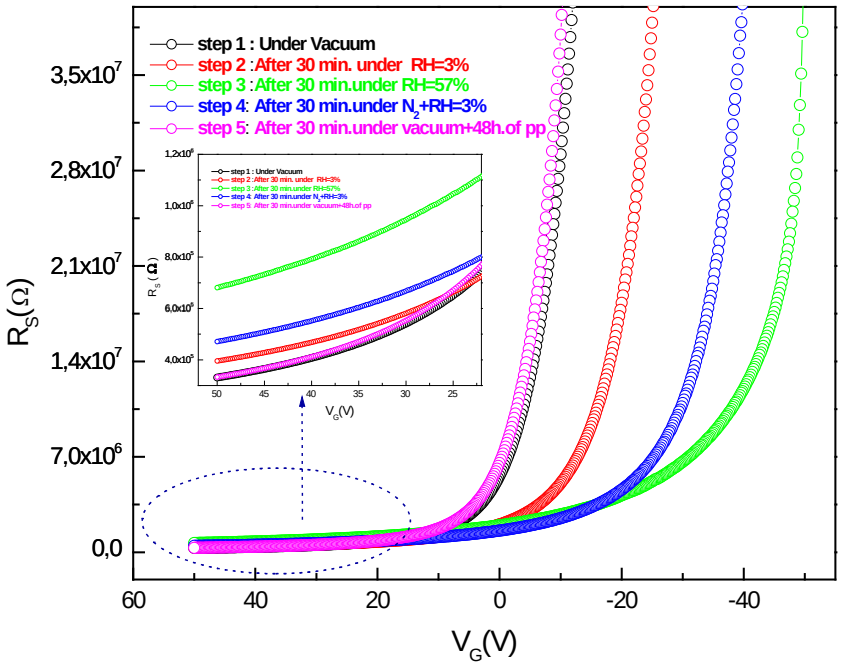
step 1 : Under Vacuum
step 2 :After 30 min. under RH=3%
step 3 :After 30 min.under RH=57%
step 4: After 30 min.under N2+RH=3%
step 5: After 30 min.under vacuum+48h.of pp
3,5x10^7
2,8x10^7
2,1x10^7
1,4x10^7
7,0x10^6
0,0
RS(Ω)
60
40
20
0
-20
-40
VG(V)

Figure.4.

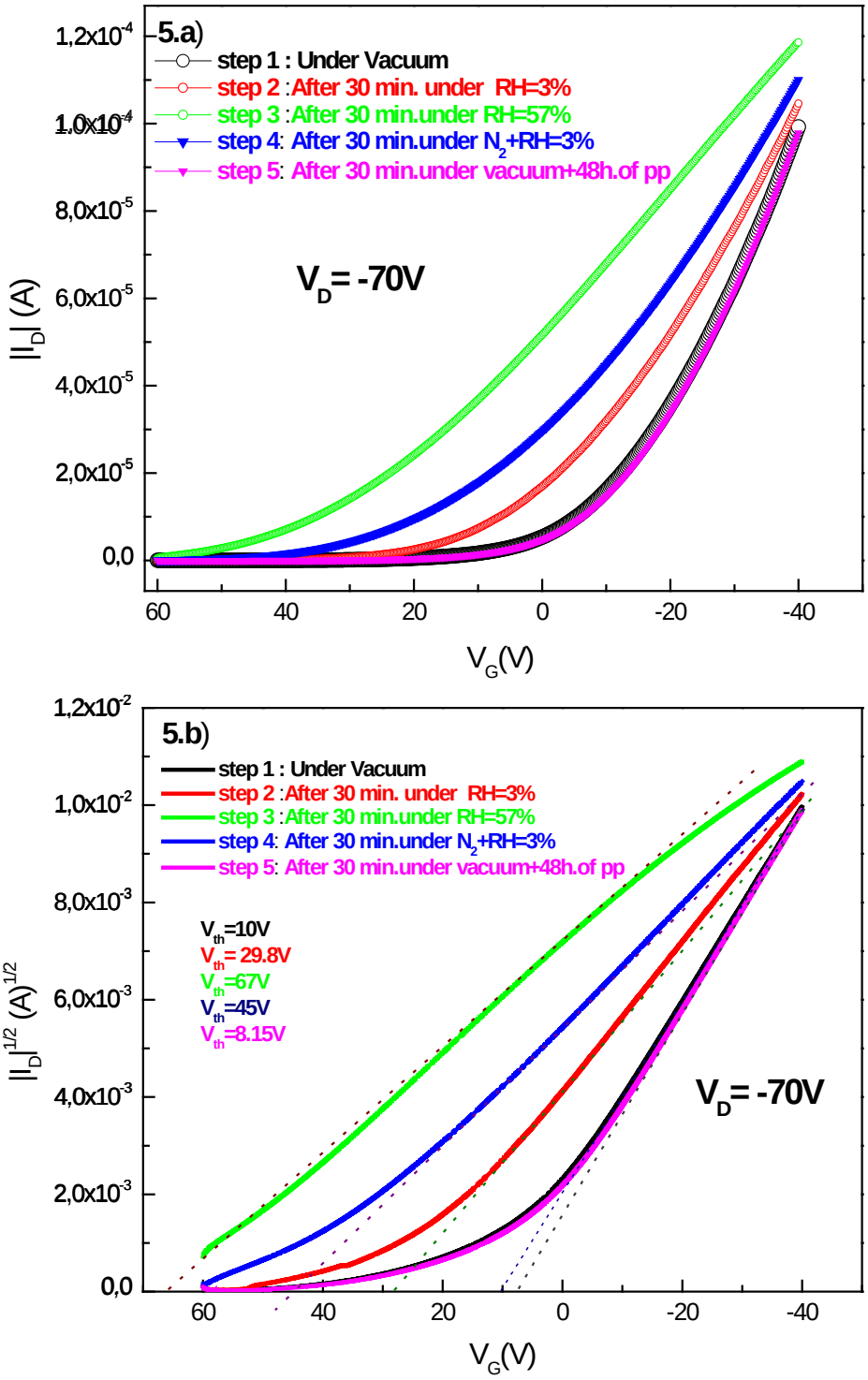
5.a)
step 1 : Under Vacuum
step 2 :After 30 min. under RH=3%
step 3 :After 30 min.under RH=57%
step 4: After 30 min.under N2+RH=3%
step 5: After 30 min.under vacuum+48h.of pp
VD= -70V
|ID| (A)
VG(V)
5.b)
step 1 : Under Vacuum
step 2 :After 30 min. under RH=3%
step 3 :After 30 min.under RH=57%
step 4: After 30 min.under N2+RH=3%
step 5: After 30 min.under vacuum+48h.of pp
Vth=10V
Vth= 29.8V
Vth=67V
Vth=45V
Vth=8.15V
VD= -70V
|ID|1/2 (A)1/2
VG(V)

Figures.5 (a)-(b).

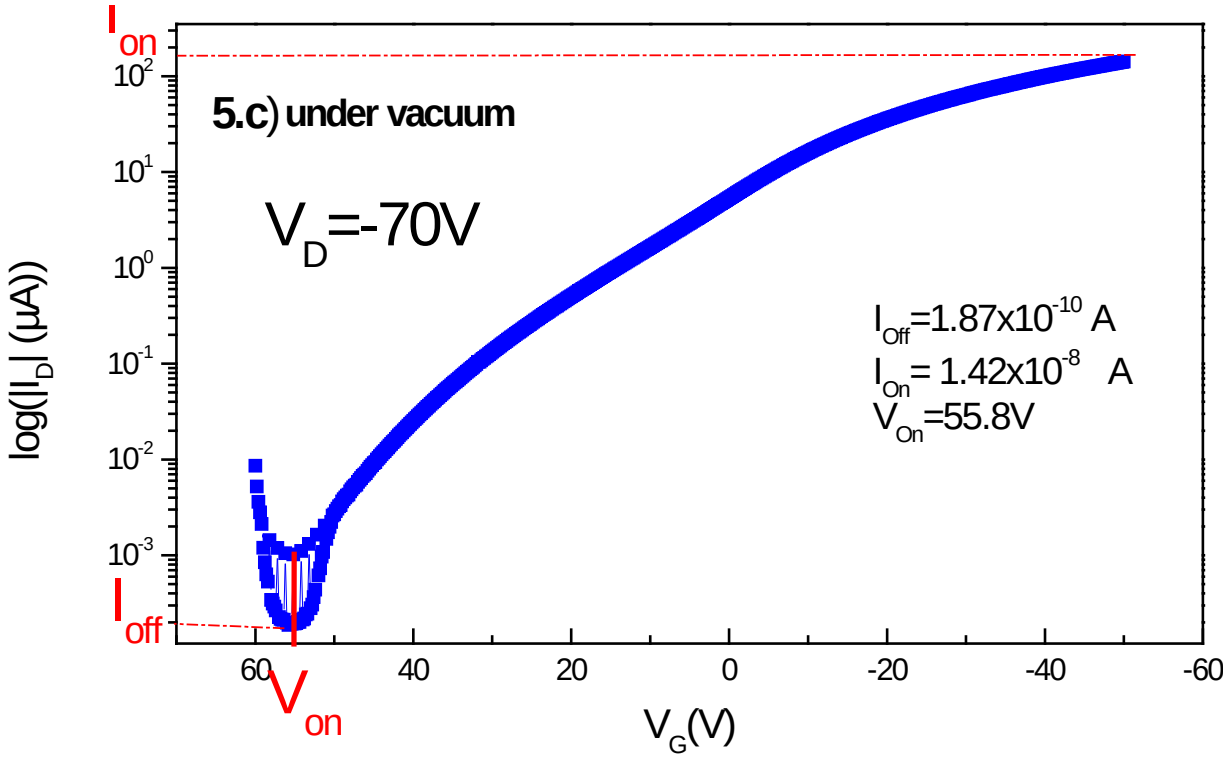
I on
10^2
10^1
10^0
10^-1
10^-2
10^-3
I off
5.c) under vacuum
V_D=-70V
I_Off=1.87x10^-10 A
I_On= 1.42x10^-8 A
V_On=55.8V
log(|I_D|) (μA))
60
40
20
0
-20
-40
-60
V on
V_G(V)

Figures.5 (c)

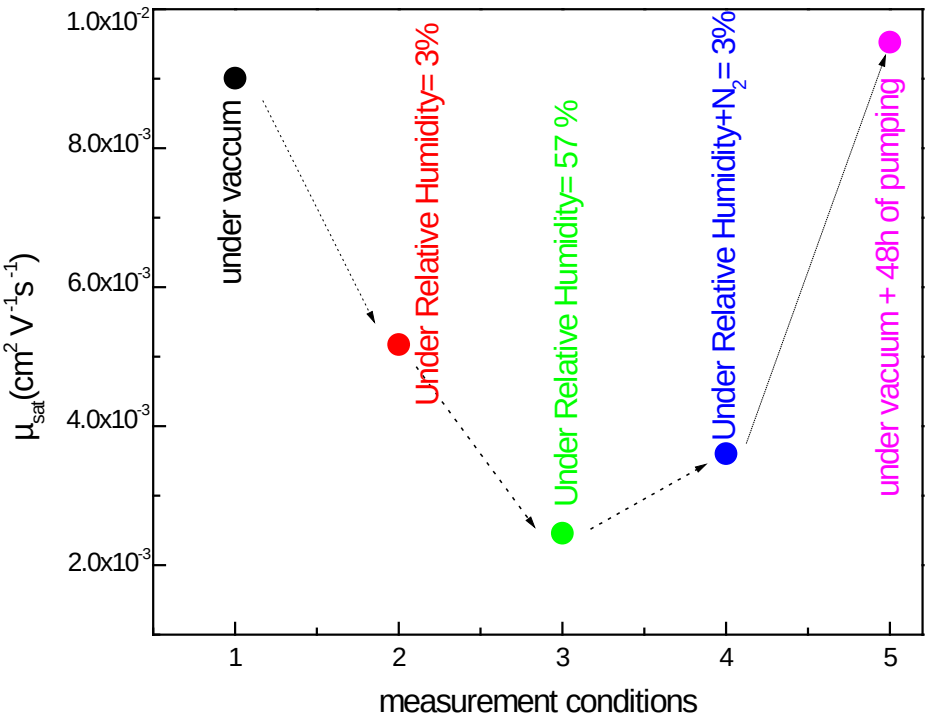
1.0x10-2
8.0x10-3
6.0x10-3
4.0x10-3
2.0x10-3
μsat(cm2 V-1s-1)
under vaccum
Under Relative Humidity= 3%
Under Relative Humidity= 57 %
Under Relative Humidity+N2= 3%
under vacuum + 48h of pumping
1
2
3
4
5
measurement conditions

Figure.6.

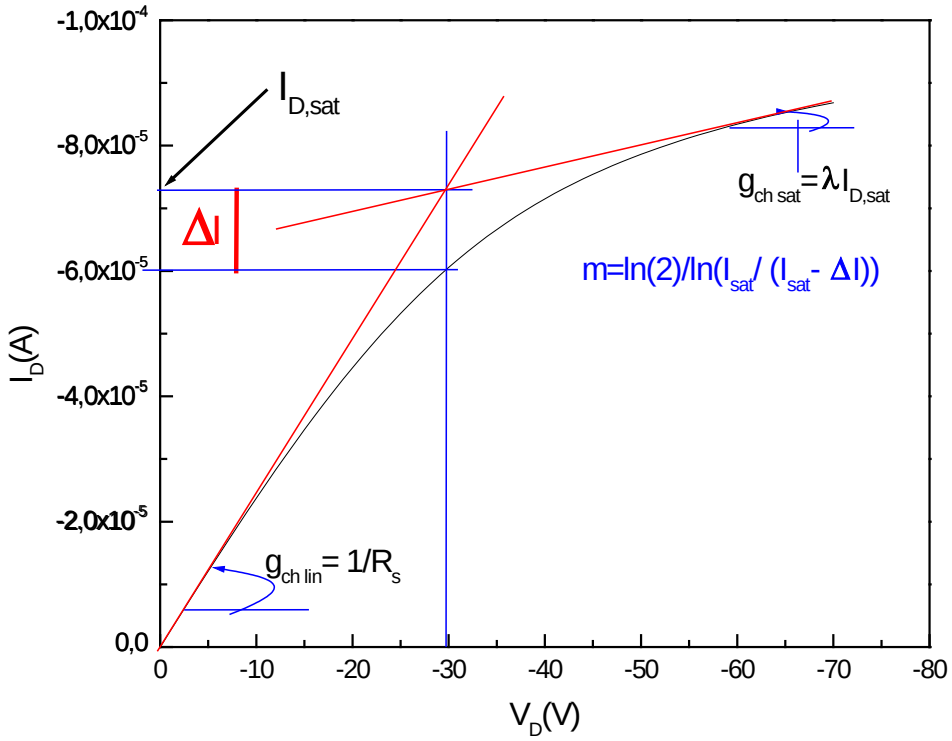
-1,0x10-4
-8,0x10-5
-6,0x10-5
-4,0x10-5
-2,0x10-5
0,0
ID(A)
0
-10
-20
-30
-40
-50
-60
-70
-80
VD(V)
ID,sat
ΔI
gch sat=λID,sat
m=ln(2)/ln(Isat/ (Isat- ΔI))
gch lin= 1/Rs

Figure.7.

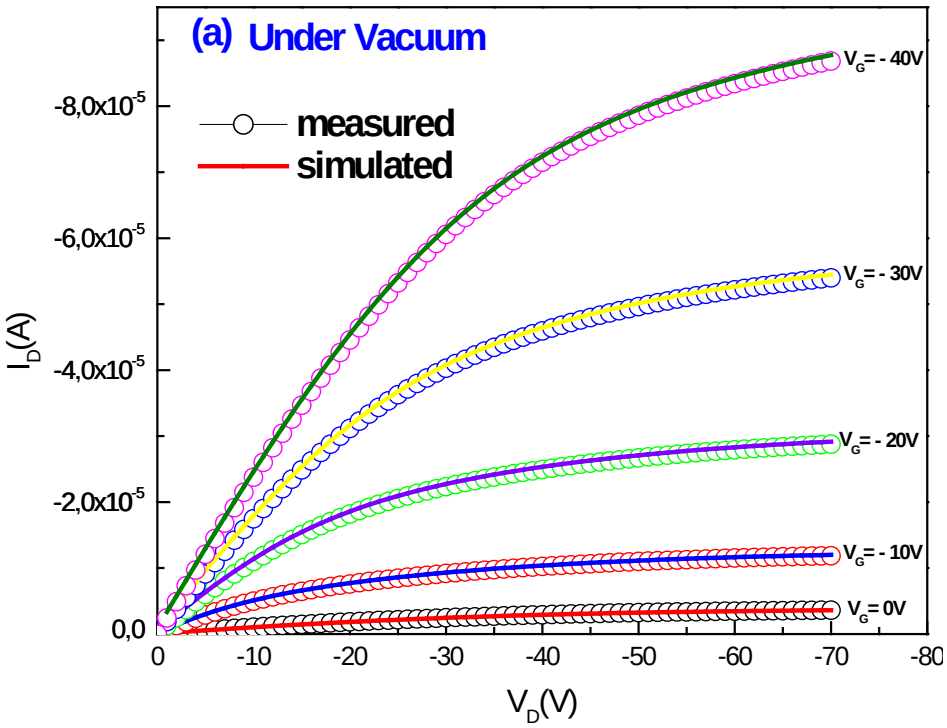
(a) Under Vacuum
measured
simulated
V_G= - 40V
V_G= - 30V
V_G= - 20V
V_G= - 10V
V_G= 0V
I_D(A)
-8,0x10^{-5}
-6,0x10^{-5}
-4,0x10^{-5}
-2,0x10^{-5}
0,0
0
-10
-20
-30
-40
-50
-60
-70
-80
V_D(V)

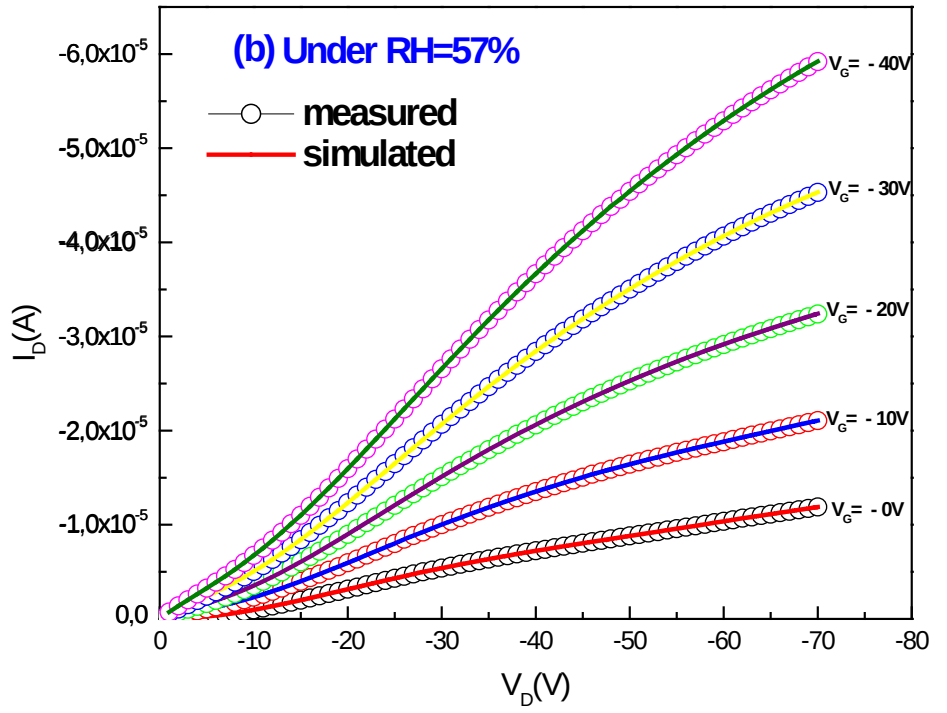
(b) Under RH=57%
measured
simulated
V_G= - 40V
V_G= - 30V
V_G= - 20V
V_G= - 10V
V_G= - 0V
I_D(A)
-6,0x10^{-5}
-5,0x10^{-5}
-4,0x10^{-5}
-3,0x10^{-5}
-2,0x10^{-5}
-1,0x10^{-5}
0,0
0
-10
-20
-30
-40
-50
-60
-70
-80
V_D(V)

Figures.8 (a)-(b).

Parameters	V_{th} (V)	$N_{trap.\ charge}$ (cm^{-2})	SS (V/dec)	D_{it} ($cm^{-2}\ eV^{-1}$)	V_{on} (V)	I_{on}/I_{off}
Under vacuum (3×10^{-5} to 5×10^{-5}mbar)	10	7.18×10^{11}	3.51	4.18×10^{12}	55.8	7.59×10^{5}
After 30min. under RH=3%	29.8	1.42×10^{12}	2.61	3.09×10^{12}	56.2	9.18×10^{4}
After 30min. under RH=57%	67	4.09×10^{12}	19.75	2.38×10^{13}	60	2.61×10^{2}
After 30min. under N_2+RH=3%	45	2.5×10^{12}	6.19	7.43×10^{12}	60	5.7×10^{3}
After 30min. under vacuum (3×10^{-5} to 5×10^{-5}mbar)**+48h of pp**	8	1.07×10^{11}	4.3	5.138×10^{12}	55	1.2×10^{6}

Table.1.

Parameters	m	λ (V^{-1})	α_s	σ_0(AV^{-1})	V_{th}(V)	R_s (Ω)	$g_{ch,\ sat}$(AV^{-1})
Under vacuum	3.48	4.88×10^{-3}	0.0854	0.78×10^{-12}	9.75	9.34×10^{6}	1.6×10^{-8}
Under RH=57%	0.238	0.02	$2\ 10^{-3}$	0.78×10^{-12}	65.9	4.22×10^{6}	1.5×10^{-7}

Table.2.